

Conference Presentation

**Aluminium sheet metal forming at low temperatures**

Schneider, R., Heine, B., Grant, R.J. and Zouaoui, Z.

This is a paper presented at the *Advanced Materials for Demanding Applications conference*, 7-9 April 2014.

Content from this work may be used under the terms of the Creative Commons Attribution 3.0 licence. Any further distribution of this work must maintain attribution to the author(s) and the title of the work, publication citation and DOI.

---

**Recommended citation:**

Schneider, R., Heine, B., Grant, R.J. and Zouaoui, Z. (2015), "Aluminium sheet metal forming at low temperatures", in IOP Conf. Series: Materials Science and Engineering, Vol.74, 012014. Proceedings of Advanced Materials for Demanding Applications conference, 7-9 April 2014, St. Asaph, UK. doi: 10.1088/1757-899X/74/1/012014

# Aluminium Sheet Metal Forming at Low Temperatures

R Schneider<sup>1,2</sup>, B Heine<sup>2</sup>, R J Grant<sup>1</sup> and Z Zouaoui<sup>1</sup>

<sup>1</sup> Glyndŵr University, Mold Road, Wrexham, LL11 2AW, UK

<sup>2</sup> Aalen University, Beethovenstr. 1, Aalen, 73430, DE

[robert.schneider.wrexham@hotmail.com](mailto:robert.schneider.wrexham@hotmail.com)

**Abstract.** Low-temperature forming technology offers a new potential for forming operations of aluminium wrought alloys which show a limited formability at ambient temperatures. This paper indicates the mechanical behaviour of the commercial aluminium alloys EN AW-5182 and EN AW-6016 at low temperatures. Stress-strain relationships at different temperatures were investigated through tensile testing experiments. Flow curves were extrapolated using an adapted mathematical constitutive relationship of flow stress and strain. A device which allows cupping tests at sub-zero temperatures was specially designed and a limiting dome height was determined.

## 1. Introduction

Statutory provisions of CO<sub>2</sub> emissions require constructive measures regarding the weight reduction of a car body. An option to reduce the nominal weight of automotive structures is to use light-weight materials, such as aluminium alloys, instead of steel [1, 2]. Commonly used aluminium alloys in the sheet metal processing industry are EN AW-5182 for interior panels and EN AW-6016 for outer skin applications. It is known that the forming behaviour for certain aluminium alloys is limited when formed at ambient temperatures [3, 4].

An option to enhance the forming behaviour of currently used aluminium alloys would be a thermal heat treatment application [5], but thermally induced forming operations may influence the mechanical behaviour of such alloys. Thus, forming aluminium alloys below room temperature would be an approach, where strain hardening losses and precipitation processes are not an issue. In this regard there is no danger of a reduction in strength through the mechanism of recovery, recrystallization and aging which is in most cases induced by forming at higher temperatures.

Based on limited published data [6-8] where the idea of improving the formability of aluminium and its alloys by a low temperature treatment is mentioned, the potential and the feasibility of such a technique is still questionable, however, in the current research, stretch forming investigations have been performed to show the applicability of the low temperature treatment for multi-axial stress states.

## 2. Experimental

### 2.1. Materials

For this study aluminium alloy sheets with the designation EN AW-5182 H111 and EN AW-6016 T4, showing a thickness of  $t = 1.15$  mm, were used. Table 1 illustrates the composition specification of tested aluminium alloys.



**Table 1.** Chemical composition of tested aluminium alloys (wt.-%)

	Si	Fe	Cu	Mn	Mg	Cr	Zn	Ti
AA5182	0.20	0.35	0.15	0.35	4.40	0.10	0.25	0.10
AA6016	1.20	0.40	0.15	0.15	0.40	0.10	0.15	0.15

### 2.2. Laboratory

The experiments were performed using a tensile testing machine from Zwick with a 100 KN loading cell. For data processing the software package testXpert V 11.0 was used. The set-up shown was implemented into the tensile testing machine where forces and displacements could be monitored.

#### Tensile tests:

Flat sheet specimens were CNC machined showing a test section width of 12.5 mm in accordance with DIN EN ISO 6892-1 ( $A_{50}$ ) [9]. Attention was given towards the rolling direction of the sheet metal which was perpendicular to the applied load. The length of the 50mm wide clamp sections of the specimens were designed to fit with the requirements of the cryogenic set-up. A specially designed cryogenic dewar, Figure 1, was used to obtain and maintain the sub-zero temperatures required in these tests. A variation of testing temperatures was reached by way of a *medium-pipe*, which was used as a vessel carrying isothermal media, and was cooled by liquid nitrogen ( $LN_2$ ). The final temperature was reached in the cryogenic dewar, where the specimen remained for around 5 minutes, before the test started. Furthermore, homogeneity of the temperature within the medium-pipe was accomplished by injecting inert gas. In case of a sudden temperature drop the chamber included an inlet for compressed air, which ensured a replacement of the cold environment between medium-pipe and cryogenic dewar. The tensile tests were conducted at five different temperatures of 25, -50, -100, -150, and -196 °C with a forming velocity of  $v_f = 200$  mm/min (maximum velocity of the tensile testing machine) resulting in a strain rate of  $\dot{\epsilon}_f(v_f) = 6.60 \times 10^{-2} \text{ s}^{-1}$ .

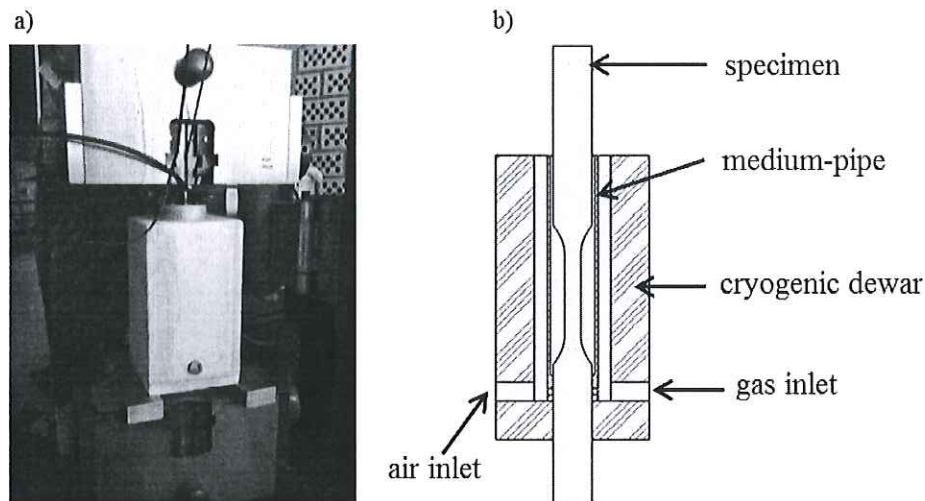


**Figure 1.** a) Tensile test equipment; b) cross-sectional view of tensile test set-up.

#### Limiting dome height (LDH):

A stretch forming apparatus capable of operating at very low temperatures was designed for evaluating the LDH (Fig. 2).  $LN_2$  was used for cooling the apparatus to sub-zero temperatures. The temperature

was monitored via thermocouples placed at the punch, blank holder, die, and blank. A cross-sectional view of the geometry used in the tests is shown in Fig. 2b which is based on [10]. Pre-investigations showed that by using graphite based anti-friction agents a moderate lubrication of the system is still achieved at low temperatures. Thus, both sides of the quadratic blank ( $100 \times 100$  mm) were wetted using graphite suspension before forming. Afterwards, the blanks were cooled to the desired forming temperature inside the testing apparatus via conductivity. Constraining the flow of the blank material into the die was achieved by tightening six carriage bolts positioned in a circle, Figure 2a. As a stop criterion for the test a punch load-drop of 50 N was taken as an indication of necking in the specimen. The punch velocity was set to be  $v_p = 50$  mm/min. For statistics five experiments were carried out at each temperature level.

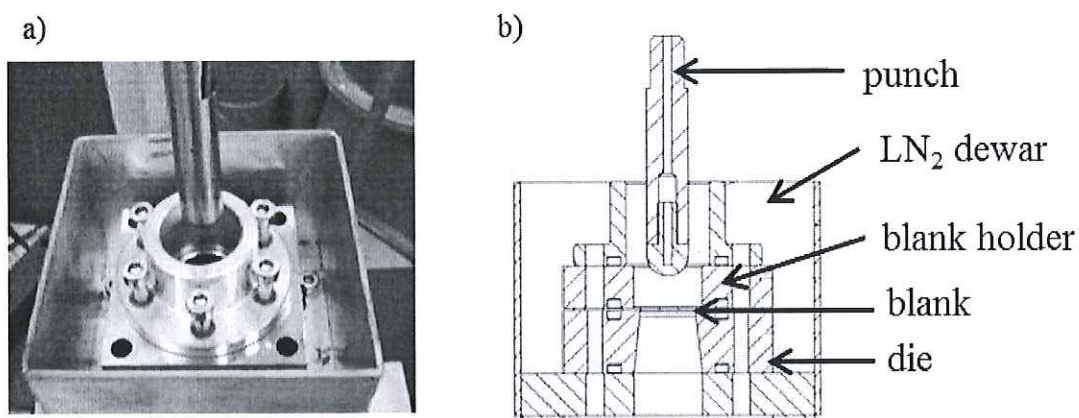


**Figure 2.** a) Low temperature stretch forming apparatus; b) Cross-sectional view of LDH set-up.

### 3. Results and Discussion

#### 3.1. Effect of temperature on strength and ductility

Figure 3 shows the true stress-strain relationship of AA5182 and AA6016 at different temperatures. It can be seen that a reduction in temperature has a positive effect on the total strain values. The strain values from AA5182, Figure 4a, rise from initially 0.24 at  $25^{\circ}\text{C}$  to 0.43 at  $-196^{\circ}\text{C}$ , which is an overall increase of 75%. A similar behaviour can be noticed for AA6016 (Fig. 3b), where the initial strain of 0.24 at  $25^{\circ}\text{C}$  could be enhanced by 42% at  $-196^{\circ}\text{C}$  and reached a total strain value of 0.34. Furthermore, the true stress rises noticeably when temperature is lowered. The phenomenon of optimizing the stress-strain behaviour at low temperatures is based on the suppression of the thermal nature of cross-slip, which results in a higher strain hardening rate and therefore strain values can be increased [11-13].

#### 3.2. Mathematical formulation of the flow stress

Ludwik, Hollomon, and Backofen identified that the flow stress  $\sigma_f$  can be elevated by raising the strain  $\varepsilon$  as well as lifting the strain rate  $\dot{\varepsilon}$  [14]. The general relationship between the physical values is given by the equation:

$$\sigma_f = \sigma_f(\varepsilon, \dot{\varepsilon}) \quad (1)$$

A relationship which was empirically developed by Ludwik modified by Hollomon and extended by Backofen [15] has the form:

$$\sigma_f = C_0 \cdot \varepsilon^n \cdot \dot{\varepsilon}^m \quad (2)$$

Where  $C_0$  is a material dependent constant (strength coefficient),  $n$  being the strain-hardening coefficient and  $m$  represents the strain rate sensitivity parameter. At temperatures where a metallurgical softening takes place to a limited extent ( $T \leq 0.4T_m$ ;  $T_m$  = melting point [K]), an increase of the strain rate will not affect the true stress. Therefore, the  $m$  value can be assumed to be much smaller than 1. If  $m$  is set to be 0 then:

$$\sigma_f = C_0 \times \varepsilon^n \quad (3)$$

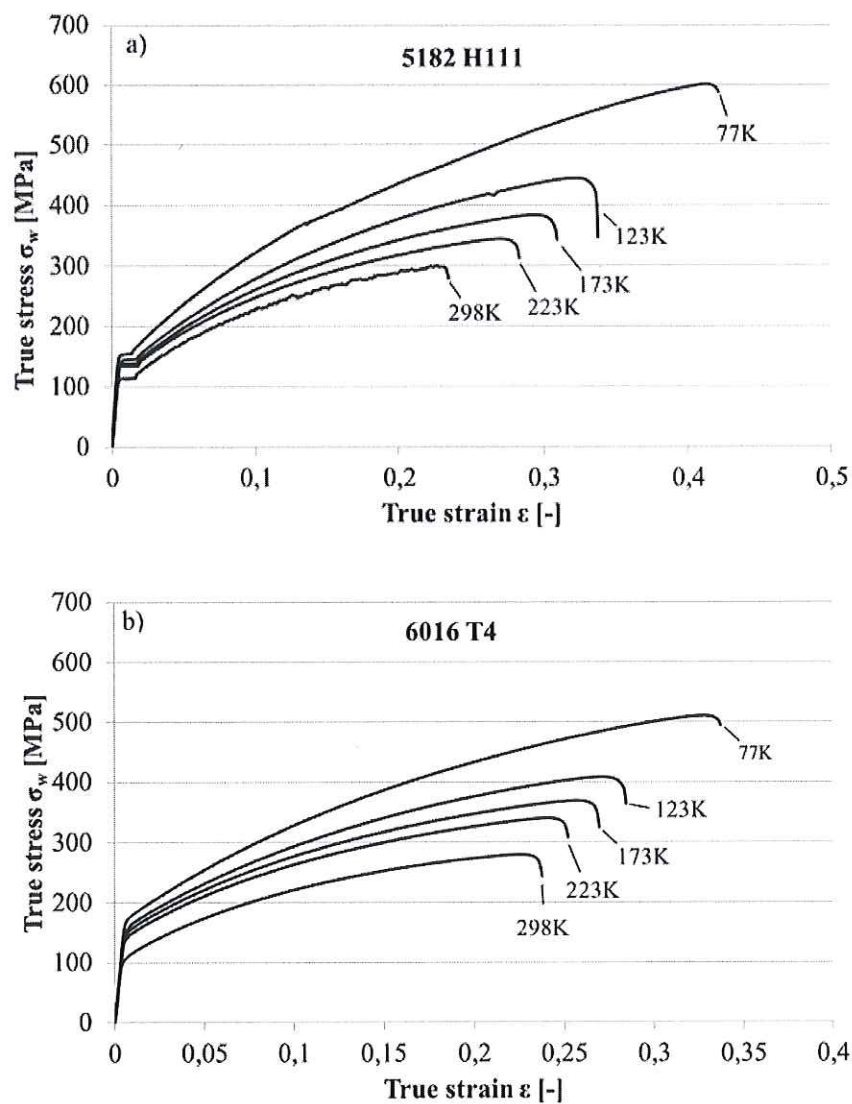


**Figure 3.** True stress–true strain diagram of a) AA5182 H111 and b) AA6016 T4 at different temperatures.

Using this relationship most stress-strain curves can be described accurately in the region of uniform elongation at  $T \leq 0.4T_m$ . As exemplified in Heiser [16] the strain hardening coefficient  $n$  can be written as true uniform strain  $\varepsilon_u$  or related to the uniform elongation  $e_u$ .

$$n = \varepsilon_u = \ln(1 + e_u) \quad (4)$$

The strain hardening coefficient  $n$  describes to what extent a material can be deformed before localised necking will start, *i.e.* the flow curve. Figure 4 shows correlations between experimental evaluated strain hardening coefficients using Equation (4) and uniform elongation  $e_u$  in relation to temperature of EN AW-5182 H111 and EN AW-6016 T4 specimens. In addition, the Ludwik curve is included which represents  $n$  calculated using Equation (4).

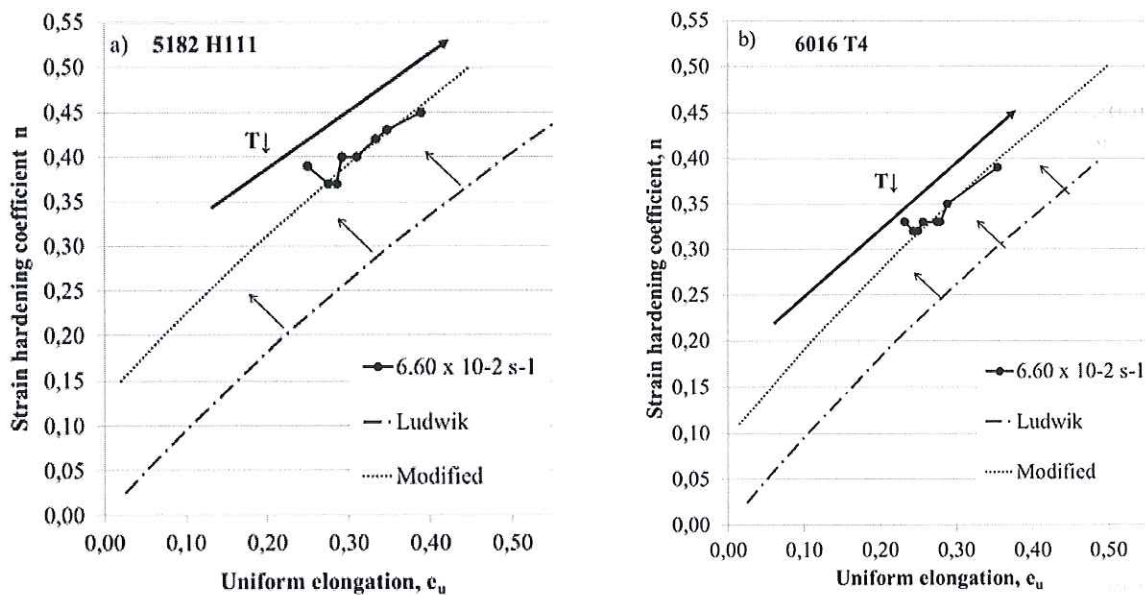


**Figure 4.** Strain hardening exponent  $n$  and uniform elongation  $e_u$  for a) AA5182 H111 and b) AA6016 T4. Additionally included is the dependence of strain hardening coefficient and uniform elongation after Ludwik if only strain hardening is considered.

Both aluminium alloys show an increase of the strain hardening coefficient and uniform elongation as temperature is reduced, Figures 4a and 4b. Furthermore, a parallel offset from the initial Ludwik curve can be noticed. Thus, Equation (3) seems not to be precisely enough for tested aluminium alloys. A modification to this equation is indicated by Equation (5), where constant  $p$  is added, which provides a shift of the Ludwik curve shown in Figures 4a and 4b.

$$n = \ln(1 + e_u) + p \quad (5)$$

If Equation (5) is put into Equation (3) it follows that:

$$\sigma_f = C_0 \times \varepsilon^{n-p} \quad (6)$$

Figure 5 shows the correlation of experimental obtained flow curves (EN AW-5182 and EN AW-6016) and the respective flow curve approximations using the extended formulation, Equation (6).

The constant  $p$  is determined by using a target value search algorithm, where the error total of the flow curve approximation is minimised.

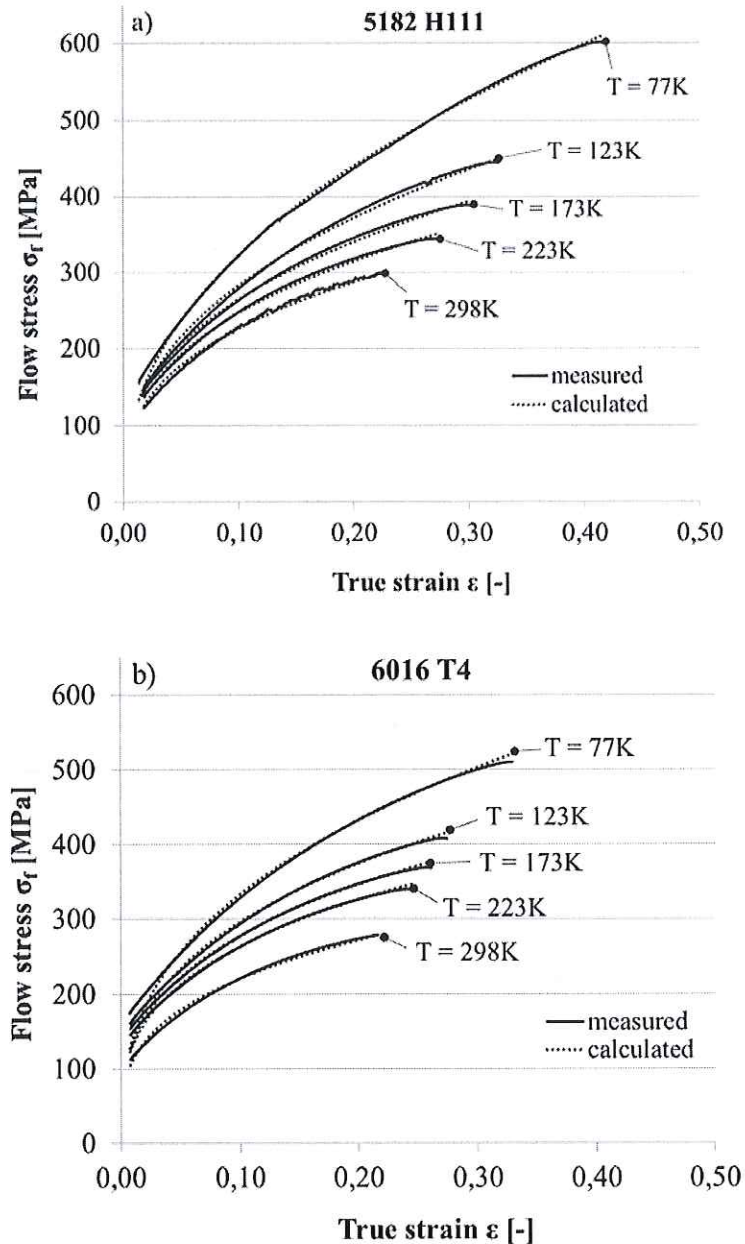


**Figure 5.** Correlation of measured and calculated flow curves at various temperatures for a) AA5182 H111 and b) AA6016 T4.

### 3.3. Limiting dome height (LDH) $D_h$

Figure 6 shows the relationship between limiting dome height and temperature for tested aluminium alloys. Similar to the tensile tests the EN AW-5182 shows an increase in formability if temperature is decreased. From 298 K to 173 K there is no significant change of the dome height. The  $D_h$  value rises

notably between 173 K and 77 K. The initial dome height at room temperature can be increased by 20% when the EN AW-5182 material is exposed to 77 K. A different behaviour, concerning LDH, shows the EN AW-6016 material when temperature is lowered. It can be seen that the formability behaviour declines between 298 K and 123 K. Only at 77 K the initial  $D_h$  value could be surpassed by around 2%, therefore, EN AW-6016 shows limitations in the formability at hydrostatic stress conditions when temperature is decreased.

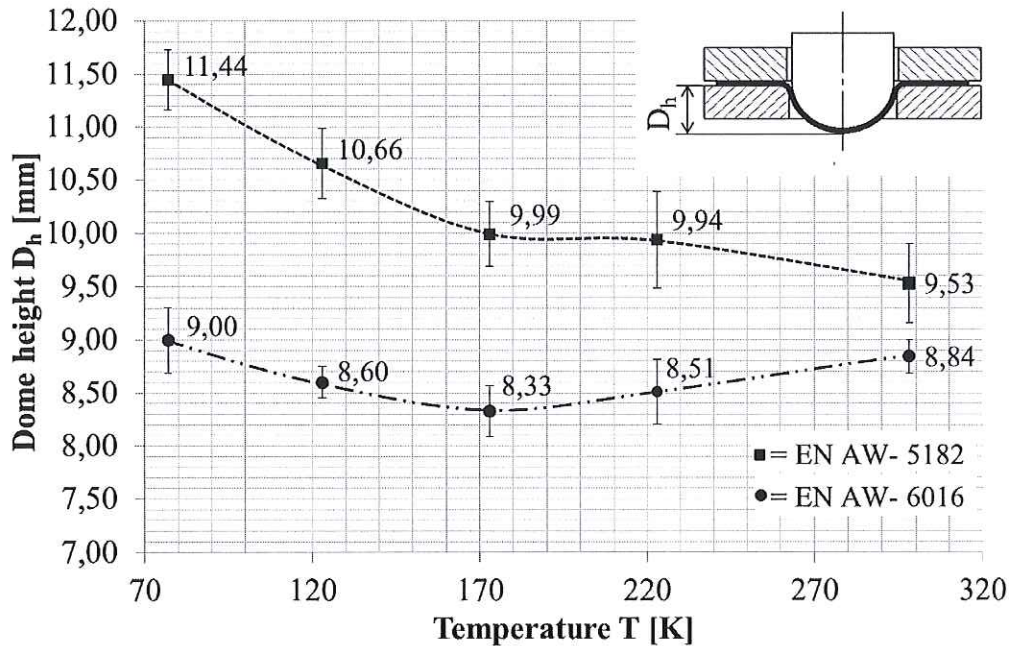


Figure 6. Limiting dome height of EN AW-5182 and EN AW-6016 at different temperatures.

#### 4. Conclusion

Tensile testing at low temperatures showed an increase of elongation values for both tested aluminium alloys EN AW-5182 H111 and EN AW-6016 T4. Corresponding stress values rise as temperature is decreased. The flow curves obtained at sub-zero temperatures can be approximated quite accurately by an adapted stress-strain relationship based on the model proposed by Ludwik and Hollomon. LDH tests showed that the stretch formability of EN AW-5182 can be enhanced at temperatures below 298K which is comparable to the conducted tensile tests. A different behaviour than that found in uniaxial tensile testing can be noticed for EN AW-6016 for biaxial stress conditions as temperature was lowered, which limits the low temperature potential for this alloy.

#### References

- [1] Wang H, Luo Y-B, Friedman P, Chen M-H and Gao L 2012 *Trans. Non. Met. Soc.* **22** 1-7.
- [2] Dössel K-F 2013 *J. Oberfl.* **53-3** 20-24.
- [3] Pink E and Grinberg A 1984 *Aluminium* **60** 764.
- [4] Pink E and Grinberg A 1984 *Aluminium* **60** 687.
- [5] Hogg M 2006 *Herstellung und Umformung lokal wärmebehandelter Platinen* vol 53, ed Siegert K and Liewald M, DGM Informationsgesellschaft mbH, Frankfurt.
- [6] Reed R P and Clark A F 1983 *Materials at low temperatures*, ASM, Ohio.



- [7] Ekin J W 2007 *Experimental Techniques for Low-Temperature Measurements*, University Press, Oxford.
- [8] Aluminium standards and data 1976 Congress no 74-83459, Aluminium Association, New York.
- [9] DIN ISO 6892-1 2009 *Metallische Werkstoffe - Prüfverfahren bei Raumtemperatur*, Beuth-Verlag, Berlin.
- [10] DIN ISO 20482 2013 *Metallische Werkstoffe - Bleche und Bänder - Tiefungsversuch nach Erichsen*, Beuth-Verlag, Berlin.
- [11] Wigley D A 1971 *Mechanical Properties of Materials at Low Temperatures*, Plenum, New York.
- [12] Seeger P H A 1958 *Phil. Mag.* **3** 470.
- [13] Nabarro F R N 1989 *Act. Met.* **37** 1521-1546.
- [14] Gregory J K 1983 *Superplastic deformation in oxide dispersion strengthened nickel base superalloys*, University Press, Stanford.
- [15] Heine B 2011 *Werkstoffprüfung Ermittlung von Werkstoffeigenschaften* (München: Carl Hanser).
- [16] Heiser M and Lange G 1992 *Z. Met.* **83** 115